Research Article

Ke-lin Zhang, Kai-ming Wu*, Oleg Isayev, Oleksandr Hress, Serhii Yershov, Vladimir Tsepelev, and Cheng-yang Hu*

Effects of different deoxidization methods on high-temperature physical properties of high-strength low-alloy steels

https://doi.org/10.1515/htmp-2020-0050
received April 21, 2019; accepted March 25, 2020

Abstract: This study was aimed at examining the effects of different deoxidization methods on the physical properties of metallic melts by measuring the changes in the kinematic viscosity, electrical resistivity, surface tension, and density of the metallurgical melts during the heating and cooling processes. Our results indicate that high-temperature physical properties are consistently affected by specific elements and compounds.

Keywords: liquid steel, kinematic viscosity, surface tension, electrical resistivity, density

*** Corresponding author: Kai-ming Wu,** The State Key Laboratory for Refractories and Metallurgy, Hubei Province Key Laboratory of Systems Science in Metallurgical Process, International Research Institute for Steel Technology, Collaborative Innovation Center for Advanced Steels, Department of Applied Physics, Wuhan University of Science and Technology, Wuhan 430081, China, e-mail: wukaiming@wust.edu.cn, tel: +86 27 68862772, fax: +86 27 68893261

*** Corresponding author: Cheng-yang Hu,** The State Key Laboratory for Refractories and Metallurgy, Hubei Province Key Laboratory of Systems Science in Metallurgical Process, International Research Institute for Steel Technology, Collaborative Innovation Center for Advanced Steels, Department of Applied Physics, Wuhan University of Science and Technology, Wuhan 430081, China; Laboratory for Excellence in Advanced Steel Research, Department of Metallurgical, Materials and Biomedical Engineering, University of Texas at El Paso, El Paso, TX 79968, USA, e-mail: chu@miners.utep.edu

Ke-lin Zhang, Oleg Isayev, Oleksandr Hress, Tsepelev Vladimir: The State Key Laboratory for Refractories and Metallurgy, Hubei Province Key Laboratory of Systems Science in Metallurgical Process, International Research Institute for Steel Technology, Collaborative Innovation Center for Advanced Steels, Department of Applied Physics, Wuhan University of Science and Technology, Wuhan 430081, China

Yershov Serhii: Research Center on Liquid Metal Physics, Department of Physics, Yeltsin Ural Federal University, Yekaterinburg 620000, Russia

1 Introduction

Numerous physical and chemical reactions, occurring during metallurgical smelting and ingot casting, are found to be closely related to the physicochemical properties of the molten metal. Reactions (decarbonization, dephosphorization, desulfurization, and deoxidization), removal of non-metallic inclusions, and segregation of various elements during the steel-making process are correlated with the viscosity, surface tension, and diffusivity of elements in the molten steel. Notably, the physical properties of the molten metal also lay an important foundation for studying its structure in the molten state in addition to the various atomic forces acting on it. Moreover, they supply a clue to investigate the following phenomena at high temperatures: the amorphous formation ability, interactions between impure elements and metallurgical vessels, deep removal of non-metallic oxides, existing forms of oxides in the molten steel, and the impact of oxides on the properties of iron-based materials [1,2]. Therefore, it is of crucial importance to examine the physicochemical properties of the melts. However, only a few studies are available on this topic, which explains the complex nature of melts and the difficulties in conducting experiments on them. Although some scholars have systematically conducted studies on some two- and three-element systems [3–8], reports describing the complex composition have not been found. Tyagunov et al. [9] have explored several high-temperature physical properties. However, there are several conflicts among their results. Thus, many questions do still remain unanswered.

Previous studies have indicated that Zr-killed steel is superior in numerous aspects when compared with Al-killed steel [10–13]. In particular, the steel produced by the Zr-killed technique has been found to exhibit superior strength, elongation, ductility, and impact toughness without obvious anisotropy when compared with Al-killed steel. Besides, the density of coarse inclusions in Zr-killed steel (mainly consisting of spherical oxide inclusions

($x\mathrm{ZrO_2}$–$y\mathrm{CaO}$–$z\mathrm{Al_2O_3}$)) is lower than that of Al-killed steel (mainly consisting of elongated MnS, coarse TiN, and string $x\mathrm{CaO}$–$y\mathrm{Al_2O_3}$). Generally, the differences in the number and nature of inclusions can determine the mechanical properties of steel. The lattice constants of $\mathrm{ZrO_2}$ and MnS are similar, implying that the fine $\mathrm{ZrO_2}$ particles can serve as nucleation sites to promote MnS precipitation, modify the elongated MnS, and string the $x\mathrm{CaO}$–$y\mathrm{Al_2O_3}$ inclusions.

Therefore, considering the above-mentioned points, it becomes necessary to further investigate the effects of the deoxidization process on the metal melts by measuring their high-temperature physical properties. Such a study may shed light on the potential correlations among the properties of metals both in their liquid and solid states and the role of oxides in them.

2 Experiment

2.1 Materials

Two high-strength low-alloy steel plates (A and B) were obtained from industrial trials. Steel A was produced by the Zr-killed technique, while steel B was produced by the Al-killed technique. Except for the difference in the deoxidation process, the parameters were similar for these two steels during the industrial trials. The liquid steel was treated by the following processes: basic oxygen furnaces, ladle furnace, Ruhrstahl Heraeus degassing, and thermo-mechanically controlled processing. Following this, the samples were cut from the final product directly without normalizing or tempering treatment. The chemical composition of the two steels is listed in Table 1.

2.2 Measurement of high-temperature properties

All studies were conducted in an inert atmosphere. Before conducting the experiment, the system, consisting of a metal chamber with a resistance furnace and a measuring cell with the test sample, was first evacuated to a pressure of 1.3×10^{-3} Pa, washed, and filled with purified helium to a pressure of 1.1×10^{5} Pa. In order to measure the high-temperature properties, the samples were put in a beryllium oxide crucible, heated till they melt and then heated further to 1,800°C, and finally cooled down. Each time, the temperature was raised or lowered by 30°C and kept for a duration of 10 min; the temperature was accurately maintained within the required range by a controller with an accuracy of 1°C.

The viscosity of the samples was measured by the attenuated torsional vibration method [14]. By measuring the logarithmic decrement of attenuation of the torsional fluctuations of the crucible containing the metal melt, the kinematic viscosity was calculated according to the Shvidkovsky equation. The density and surface tension were measured by the sessile drop method [15]. After the sample was melted, a droplet was formed. The light source projected the outline of the droplet onto the imaging system to take photos at the set temperature and time. From the photos of the droplet, the surface properties were calculated by a self-developed computer software. The basic principle of the software is based on the Laplace equation; the software uses an iterative method to fit the droplet profile and calculates the density, surface tension, and contact angle. Figure 1 shows the photos of samples A and B when they are about to completely melt and when they reach a temperature of 1,750°C. The contactless induction method of the rotating magnetic field was used for the resistivity measurement [16]. The working principle of the method is as follows: the specimen in the crucible is inserted in a rotating magnetic field. Field lines thread the specimen that is put on an inductive current. The magnitude of the current depends on the specimen's conductivity. The inductive currents, in turn, create an internal magnetic field that interacts with the external magnetic field. A torque acts on the specimen and gets transferred to the suspended elastic thread. As a result, the specimen turns by an angle φ with respect to its starting position. The magnitude of the angle φ depends on the electrical resistivity of the specimen, its size, rotating magnetic field induction, B, its frequency, ω, and the elasticity coefficient of the thread.

Table 1: Chemical composition of steels A and B

No.	C	Mn	P	S	Si	Ni + Cr + Cu	Al	Nb	Zr + Ti	Remarks
A	0.06	1.30	0.010	0.001	0.16	0.68	0.023	0.028	0.025	Zr killed
B	0.06	1.34	0.010	0.001	0.21	0.74	0.032	0.030	0.014	Al killed

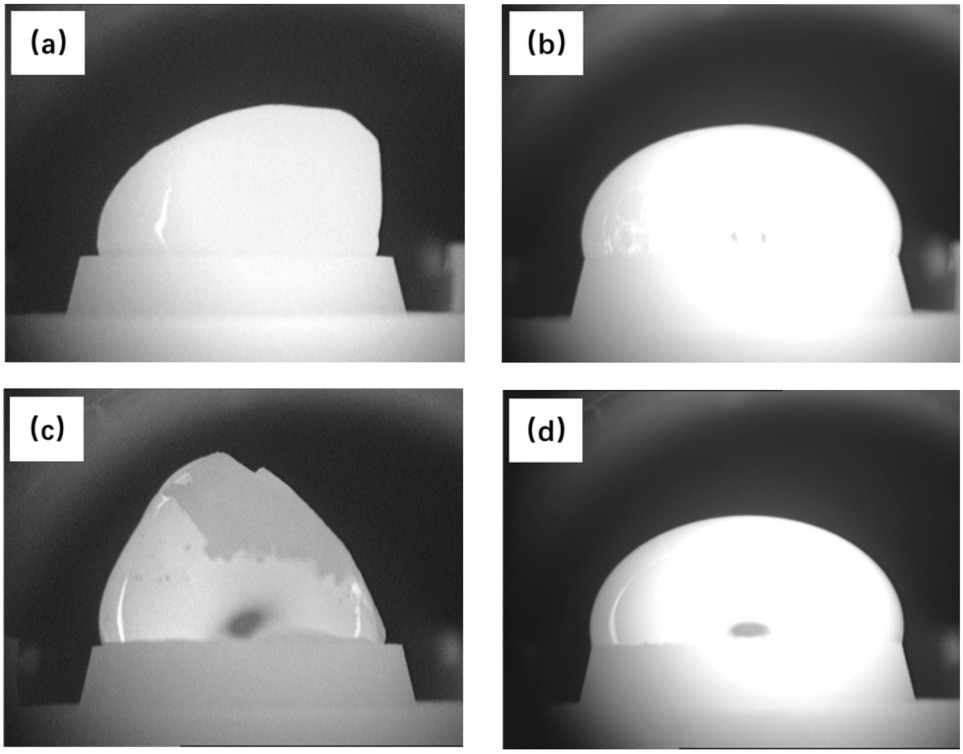

Figure 1: Photos of a droplet of sample A at temperatures of (a) 1,460°C and (b) 1,750°C and that of a droplet of sample B at temperatures of (c) 1,450 and (d) 1,750°C.

3 Results

3.1 Density

The densities of the investigated samples at different temperatures are plotted in Figure 2. The results reflect a similar tendency for both samples. First, the density increases to the maximum value and then decreases to the terminal value during the heating process. This variation is more obvious for sample B. Second, the density increases and remains stable during the cooling process when compared with the heating process at the same temperature and their differences become greater with decreasing temperature. The subtle difference is that the density of sample B is greater than that of sample A when the temperature drops below 1,670°C during the cooling process.

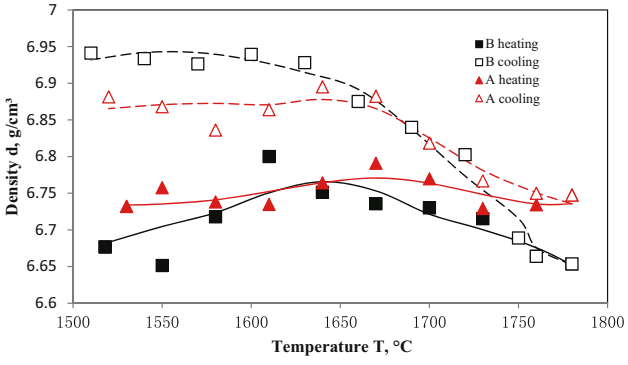

Figure 2: Changes in the density of samples A and B as a function of temperature.

3.2 Viscosity

Figure 3 illustrates the changes in the viscosity with temperature. The heating and cooling curves of both samples A and B intersect, which indicates that the viscosity of the samples during the heating and the cooling processes is very close. Both samples present a similar tendency: the viscosity decreases during the heating process and increases during the cooling process. However, there are still some subtle differences between these two samples. This decrease is much sharper for sample A when compared with sample B during the heating process, and the viscosity of sample B is greater after heating it above 1,720°C. When the temperature drops below 1,760°C during the cooling

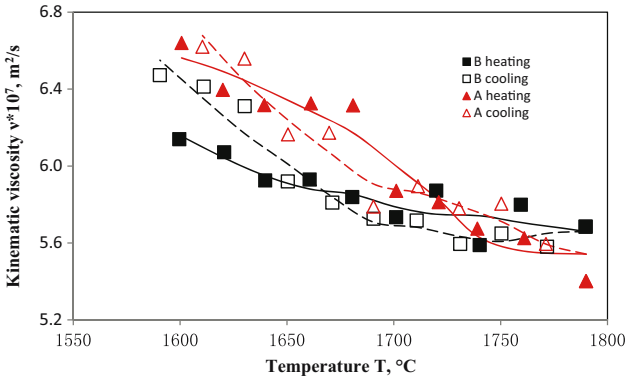

Figure 3: Changes in the kinematic viscosity of samples A and B as a function of temperature.

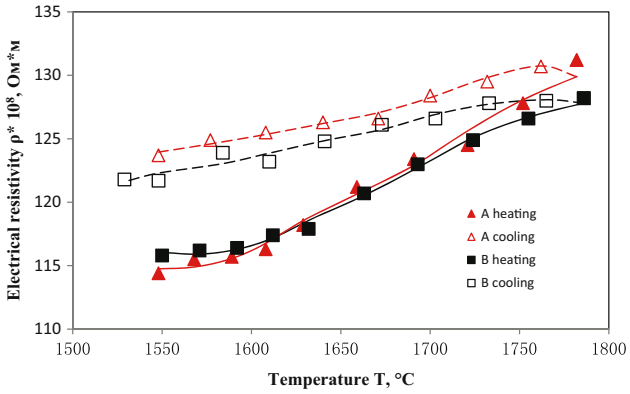

Figure 4: Changes in the electrical resistivity of samples A and B as a function of temperature.

process, the viscosity of sample A is greater than that of sample B.

3.3 Electrical resistivity

The common trend for the two samples is that the resistivity increases during the heating process and decreases during the cooling process, as shown in Figure 4. The resistivity of sample A rises more rapidly during the heating process and exceeds that of sample B at a temperature >1,610°C. The resistivity of both samples is similar during the heating process; however, sample A exhibits a higher resistivity when compared with sample B during the cooling process. The resistivity of the two samples during cooling is higher than that of the heating process at a given temperature, and this difference becomes larger with decreasing temperature.

3.4 Surface tension

As shown in Figure 5, there are obvious differences in the trend for both samples. The surface tension of sample B rises to a maximum value and then decreases during the heating process; however, it remains stable during the cooling process. As for sample A, the profile curves are more complex when compared with sample B: the surface tension drops to a minimum value showing fluctuations with increasing temperature during the heating process, while during the cooling process, it further drops to a minimum value and shows fluctuations with temperature. The surface tension of sample B stays higher than that of sample A during both the heating and cooling processes at the same temperature. The only similar part is that the surface tension of the two samples measured during the cooling process is always lower than that during the heating process.

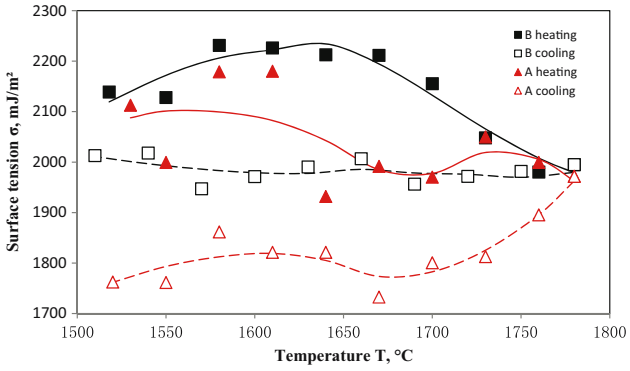

Figure 5: Changes in the surface tension of samples A and B as a function of temperature.

4 Discussion

4.1 Density

The densely arranged structure of metals, consisting of the body-centered and face-centered cubic lattices in the solid-state, retains its original structure while melting and its density decreases by only 1%–7%, due to the decrease in the atomic ordering and the increase in vacancies.

A previous report [17] gives the relationship between the liquid density and temperature of pure iron, as given in equation (1):

$$\rho_T = 8580 - 00853T \ (\mathrm{kg/m^3}). \quad (1)$$

When the temperature changes from 1,873 to 2,073 K (1,600–1,800°C), the density of pure iron decreases from 7.0 to 6.8 g/cm^3, which is higher than that of both samples. The density of molten iron is related to not only the temperature but also the type and concentration of the dissolved elements. Among the elements dissolved in molten iron, W and Mo can increase its density, Al, Si, Mn, P, and S can reduce its density, and transition metals, such as Ni, Co, Cr, and Nb, have little effect [17]. Since sample A has a lower Al, Si, and Mn content, it is denser during the heating process.

The curve branching phenomenon was observed in some previously published works. Popel [18,19] proposed the conservation of micro heterogeneity in the melt. He pointed out that there is a temperature, T-hom, above the liquidus temperature, T-L, and that the liquid steel is in a metastable state between T-L and T-hom. Only when the temperature is higher than T-hom can it change the system into a real solid solution state. The experimental temperature range in this work is between T-L and T-hom. There are many colloidal particles (1–10 nm) in the metastable state of molten steel. These colloidal particles are the ones that keep the density stable during temperature fluctuations and prevent the cooling curve from approaching the heating curve. However, the introduction of the surface-active elements (Si and Mn) reduces the interfacial tension of the colloidal particles, and thus, the effect of the colloidal particles in sample A is weakened, resulting in the closer heating and cooling curves of sample A and the smaller fluctuations in the sample during heating.

4.2 Viscosity

The viscosity is related to the size, arrangement, and combination of the particles in the melt. In an alloy, because the atoms of the elements combine to form atomic clusters, this might have different effects on the viscosity. For example, for the Fe–C alloy with different C content, its viscosity and density are nonlinear. Heterogeneous atoms in a molten metal often form agglomerations, which increase the viscosity of the melt. For example, O^{2-} and S^{2-} with Fe^{2+} form agglomerations of $Fe^{2+}{\cdot}O^{2-}$ and $Fe^{2+}{\cdot}S^{2-}$, respectively. In this case, the viscosity depends on the internal friction resistance that needs to be overcome when the agglomerate moves. With an increase in temperature, the size of the agglomerate decreases, and thus, the viscosity of the melt decreases.

The effect of other elements on the viscosity of the molten iron is as follows: Ni, Co, Cr, and other elements have little effect on the viscosity of molten iron. Mn, Si, Al, P, and S can reduce the viscosity of molten iron, especially Al, P, and S, which can reduce the viscosity of molten iron greatly. On the other hand, V, Nb, Ti, and Ta can increase the viscosity of molten iron. When there are more suspended solids in the molten iron, such as Al_2O_3 and Cr_2O_3, the measured viscosity is found to be greater.

Liu [20] found that the inclusions in the samples with Ti and Zr mainly consist of Zr_xO_y, silica, Al_2O_3, and MnS. It is easy to produce oxide inclusions of Al_2O_3 in Al-killed steel. Zr is an element having a strong deoxidization ability. The oxygen concentration in molten steel can be greatly reduced by adding a small amount of Zr element in steel, and the Al_2O_3 formed in the matrix can be modified to ZrO_2. The density of ZrO_2 is 6.0 g/cm^3, which is very close to the density of molten steel mentioned in Section 4.1. This indicates that ZrO_2 does not easily float in molten steel. As Zr–Ti oxides do not easily aggregate, the amount of oxide generated in the Zr–Ti composite-deoxidized steel is more than that of Al-deoxidized steel.

In addition, in the process of steelmaking, the contact between the lining and molten steel and the thermal decomposition of the lining at high temperatures may contaminate the molten steel to a certain degree. Because of the high content of active alloy elements, such as Zr and Al, in the molten steel, the thermal decomposition and oxygen supply of the furnace lining will cause a lot of loss of these alloy elements. As a result, the chemical composition of molten steel is difficult to be controlled accurately and the content of oxide impurities is increased, which will affect the physical properties of molten steel, as well as the processing and mechanical properties of steel [21].

4.3 Electrical resistivity

Metal melts are conductors of free electrons. As the temperature rises, the motion of the ions increases, hindering the directional movement of free electrons and thus resulting in higher resistivity.

The resistivity of Fe–C melt increases with an increase in the C concentration. For a C concentration of 0 to 0.2–0.4%, the resistivity increases sharply with increasing C concentration. When the C concentration becomes >0.4%, the resistivity increases slightly with the concentration. When C exists as a positive ion in the melt, its valence electron is transferred to the $3d^6$ orbital of iron, which reduces the electron concentration that

can conduct electricity, forms many dispersed ion impurities, and increases the resistivity. Si, like C, can increase the resistivity of molten iron, but its effect is much smaller than C [22]. In the iron-based two-component system, Cu, Ni, Cr, and Al can reduce the resistivity of molten iron, while Nb, Zr, Ti, and Mn can improve the resistivity of molten iron.

The conductivity of the oxide can also affect the molten steel. ZrO_2 has a high resistivity, which leads to higher resistivity of sample A.

4.4 Surface tension

The influence of the solute elements on the surface tension of the solvent depends on the difference between the properties of the solute and the solvent. If the properties of the solute elements are similar to those of the solvent, the forces between the solute atoms and solvent atoms are roughly similar to those between the atoms themselves and the surface tension of the solvent is affected less. On the contrary, the greater the difference between the properties of the solute element and the solvent, the greater is the influence on the surface tension of the solvent. In general, the effect of metallic elements on the surface tension of molten iron is less than that of non-metallic elements. S and O are very strong surface-active substances, and hence, the presence of a small amount of S and O will greatly reduce the surface tension of molten iron. Furthermore, Mn has a huge influence on the surface tension of liquid iron, the influence of Si, Cr, C, and P is relatively small, and Ti, V, and Mo have little effect on the surface tension of liquid iron.

The mechanism of the surface tension of the solution is different from that of the pure solvent (pure metal liquid). The former constitutes a change in the interface force field caused by the adsorption of the solute particles on the surface of the solution, while the latter is the asymmetry of the force field on the liquid surface particle compared with the internal particle. At an identical temperature, the pure liquid has definite surface tension. As the temperature rises, the thermal motion of atoms strengthens and the interaction between the particles inside the bulk and on the surface of the liquid decreases, thus causing a decrease in the surface tension.

As can be seen from Figure 5, the surface tension fluctuates greatly with increasing temperature. On one hand, the thermal motion of the particles increases, the volume expands, the particle spacing increases, and the surface tension of the solution decreases with increasing temperature. On the other hand, the adsorption of the surface layer decreases and the surface tension increases slightly. Therefore, surface tension has a complicated relationship with temperature. As sample A is deoxidized by the Zr–Ti composite, a larger number of high-melting point compounds are produced in steel when compared with sample B. These compounds could move to the surface of the liquid and reduce the surface tension of liquid steel.

5 Conclusion

In this study, various high-temperature physical properties of high-strength low-alloy steels were tested in order to explore the effects of the different deoxidation techniques on their properties. The following conclusions could be drawn:

1. Different deoxidization methods lead to different compounds and compositions in the melted metals. Among them, ZrO_2 and Al_2O_3 have the most obvious effects, resulting in a greater surface tension of sample B and a greater resistivity of sample A.
2. The resistivity of the samples is positively correlated with temperature, while viscosity is negatively correlated with temperature.
3. The high-temperature physical properties of the metal melt exhibit an obvious hysteresis effect during their cooling. The density and electrical resistivity during the cooling process are higher than that during the heating process, while the surface tension exhibits the opposite trend.

Acknowledgments: The authors gratefully acknowledge support from the National Natural Science Foundation of China (U1532268, 51671149), Wuhan Science and Technology Program (Grant No. 2019010701011382), and the 111 project.

References

[1] Tsepelev, V., Y. Starodubtsev, K. M. Wu, N. Tsepeleva, and B. Semenov. Physical and mechanical properties of the amorphous and nanocrystalline alloys. *Defect & Diffusion Forum*, Vol. 382, 2018, pp. 53–57.

[2] Tsepelev, V., Y. Starodubtsev, K. M. Wu, N. Tsepeleva, and A. Taushkanova. Magnetic and mechanical properties of the

amorphous alloys. *Defect & Diffusion Forum*, Vol. 382, 2018, pp. 58–62.
[3] Wang, H. P., J. Chang, and B. Wei. Density and related thermophysical properties of metastable liquid Ni–Cu–Fe ternary alloys. *Physics Letters. Part A*, Vol. 374, No. 24, 2010, pp. 2489–2493.
[4] Guo, Z., M. Hindler, W. Yuan, and A. Mikula. Density and surface tension of liquid Bi–Cu–Sn alloys. *Monatshefte für Chemie - Chemical Monthly*, Vol. 143, 2012, pp. 1617–1622.
[5] Kobatake, H., and J. Brillo. Density and viscosity of ternary Cr–Fe–Ni liquid alloys. *Journal of Materials Science*, Vol. 19, No. 19, 2013, pp. 6818–6824.
[6] Brillo, J., I. Egry, and T. Matsushita. Density and surface tension of liquid ternary Ni–Cu–Fe alloys. *International Journal of Thermophysics*, Vol. 6, No. 6, 2006, pp. 1778–1791.
[7] Egry, I., J. Brillo, and T. Matsushita. Thermophysical properties of liquid Cu–Fe–Ni alloys. *Materials Science and Engineering A*, Vol. 6, 2005, pp. 460–464.
[8] Willner, J., G. Siwiec, and J. Botor. The surface tension of liquid Cu–Fe–Sb alloys. *Applied Surface Science*, Vol. 9, No. 9, 2010, pp. 2939–2943.
[9] Tyagunov, A. G., E. E. Baryshev, G. V. Tyagunov, V. S. Mushnikov, and V. S. Tsepelev. Polytherms of the physical properties of metallic melts. *Steel in Translation*, Vol. 4, No. 4, 2017, pp. 250–256.
[10] Hu, C. Y. Effects of steelmaking and rolling on low temperature toughness of high strength low alloy steels, *Master thesis*, Wuhan University of Science and Technology, Wuhan, China, 2018 (in Chinese).
[11] Li, Y., X. L. Wan, W. Y. Lu, A. A. Shirzadi, O. Isayev, O. Hress, et al. Effect of Zr-Ti combined deoxidation on the microstructure and mechanical properties of high-strength low-alloy steels. *Materials Science and Engineering A*, Vol. 659, 2016, pp. 179–187.
[12] Cheng, L. C., C. Xu, L. Lu, L. Yu, and K. Wu. Experimental and first principle calculation study on titanium, zirconium and aluminum oxides in promoting ferrite nucleation. *Journal of Alloys and Compounds*, Vol. 742, 2018, pp. 112–122.
[13] An, Z. Y., K. M. Wu, W. Y. Lu, H. H. Wang, X. L. Wan, and Y. K. Yao. Effect of Zr-Ti combined deoxidation on impact toughness of coarse-grained heat-affected zone with high heat input welding. *China Welding*, Vol. 4, 2014, pp. 56–62 (in Chinese).
[14] Povodator, A. M., V. S. Tsepelev, and V. V. Konashkov. Fast viscosity determination for high-temperature metal alloys. *Steel in Translation*, Vol. 45, No. 6, 2015, pp. 407–411.
[15] Tanaka, T., M. Nakamoto, R. Oguni, J. Lee, and S. Hara. Measurement of the surface tension of liquid Ga, Bi, Sn, In and Pb by the constrained drop method. *Zeitschrift fur Metallkunde*, Vol. 95, No. 9, 2004, pp. 818–822.
[16] Ryabina, A. V., V. I. Kononenko, and A. A. Razhabov. Electrodeless Method for Measuring the Electrical Resistance of Metals in the Solid and Liquid States and Apparatus for Its Implementation. *Melts*, Vol. 1, 2009, pp. 36–42.
[17] Huang, X. H. *Principles of Iron and Steel Metallurgy*, Metallurgical Industry Press, Beijing, 2002 (in Chinese).
[18] Popel, P. S. Metastable micro-heterogeneity of melts in systems with eutectic and monotectic and its effect on the alloy structure after solidification. *Rasplavy*, Vol. 1, 2005, pp. 22–48.
[19] Popel, P. S., O. A. Chikova, and V. M. Matveev. Metastable colloidal states of liquid metallic solutions. *High-Temperature Materials and Processes*, Vol. 14, No. 4, 1995, pp. 219–234.
[20] Liu, H. H. Influence of titanium and zirconium complex deoxidation on the inclusions and microstructure of steel. *Steelmaking*, Vol. 3, 2015, pp. 59–78 (in Chinese).
[21] Gao, J. B. Influence of oxygen supply caused by furnace liner on deep deoxidation of molten steel in vacuum induction melting process, *PhD thesis*, Wuhan University of Science and Technology, Wuhan, China, 2006 (in Chinese).
[22] Zhao, J. X., L. B. Li, and X. M. Li. *Metallurgical Principle*, Metallurgical Industry Press, Beijing, 2012 (in Chinese).